

Photometric and spectroscopic observations of Supernova 2014J in M82

D.Yu. Tsvetkov¹, V.G. Metlov¹, I.M. Volkov^{1,2}, S.Yu. Shugarov^{1,3}, V.P. Goranskij¹, T.N. Tarasova⁴, N.N. Pavlyuk¹, A.V. Kusakin⁵, M.A. Krugov⁵, R.I. Kokumbaeva⁵, E.A. Barsukova⁶, A.F. Valeev⁶, A.A. Nikiforova^{7,8}, I.S. Troitsky⁷ and Yu.V. Troitskaya⁷

¹ Sternberg Astronomical Institute, M.V. Lomonosov Moscow State University, Universitetsky pr. 13, 119234 Moscow, Russia

² Institute of Astronomy of the Russian Academy of Sciences, 48 Pyatnitskaya street, 119017 Moscow, Russia

³ Astronomical Institute of the Slovak Academy of Sciences
059 60 Tatranská Lomnica, The Slovak Republic

⁴ Crimean Astrophysical Observatory of the Russian Academy of Sciences,
Nauchnyi, Crimea, 298409 Russia

⁵ Fesenkov Astrophysical Institute, Almaty, Kazakhstan

⁶ Special Astrophysical Observatory of the Russian Academy of Sciences,
Nizhniy Arkhyz, Karachai-Cherkessia, 369167 Russia

⁷ Astronomical Institute, St. Petersburg State University, 198504 St.
Petersburg, Russia

⁸ Pulkovo Observatory, 196140 St.Petersburg, Russia

Received: March 30, 2018; Accepted: May 4, 2018

Abstract. We present 207 photometric epochs and 9 spectra of SN Ia 2014J in M82. *UBVRI* photometry was carried out with 13 telescopes at 8 locations, covering the period from January 23, 2014 until May 15, 2015. The parameters of the light curves and interstellar extinction are determined. The comparison of different sets of photometric data is carried out. The light and colour curves of SN 2014J are compared to those for SNe Ia with similar photometric characteristics. We present results of high-cadence monitoring of SN 2014J in the *BVR* bands carried out on 6 nights and find no evidence for the microvariability. The spectral evolution is found to be typical for SNe Ia, with the expansion velocity at the maximum slightly greater than average and with a low velocity gradient.

Key words: supernovae: individual (SN 2014J)

1. Introduction

The homogeneity and high luminosity of type Ia supernovae (SNe Ia) determine their application for measuring extragalactic distances and estimating cosmological parameters (e.g., Pskovskii, 1977; Phillips, 1993; Riess et al., 1998;

Astier et al., 2006; Kessler et al., 2009). However, the results obtained in this way are based on the assumption that distant SNe are similar to well-studied nearby objects and their luminosities can be calibrated by identical methods. At present, many fundamental questions of the physics of SNe Ia, including the nature of presupernovae and the explosion mechanism, are still not completely clear. Therefore, accumulating observational data on nearby SNe Ia and elucidating the causes of differences in their characteristics remain important tasks of modern astrophysics.

Supernova (SN) 2014J, located at $\alpha = 9^{\text{h}} 55^{\text{m}} 42^{\text{s}}.14, \delta = +69^{\circ} 40' 26''.0$ (2000.0) in the galaxy M82, was discovered by Steve J. Fossey on UT 2014 January 21.8.

At a distance of 3.5 Mpc (Karachentsev & Kashibadze, 2006) SN 2014J is the nearest SNIa after SN 1972E, and it offers the unique possibility to study a thermonuclear SN over a wide range of the electromagnetic spectrum.

The description of the discovery and early observations were presented by Goobar et al. (2014). The prediscovery data and early photometric and spectroscopic observations were reported by Zheng et al. (2014), Ashall et al. (2014), Denisenko et al. (2014), Itagaki et al. (2014), Gerke et al. (2014), Goobar et al. (2015). These sets of data show that SN 2014J is a spectroscopically normal Type Ia SN, although it exhibited high-velocity features in the spectrum and was heavily reddened by the dust in the host galaxy.

Follow-up photometric and spectroscopic observations were made by various groups, the largest sets of data are from Amanullah et al. (2014), Kawabata et al. (2014), Foley et al. (2014), Marion et al. (2015), and Srivastav et al. (2016).

Our observations for the first 40 days after the discovery were presented by Tsvetkov et al. (2014). In this paper we report the results of further extensive monitoring of SN 2014J in the optical bands carried out with 14 telescopes at 8 sites.

2. Observations and data reduction

CCD photometry of SN 2014J in the *UBVRI* passbands was carried out at:

- Nauchnyi in Crimea, where telescopes operated by the Crimean Astrophysical Observatory (CrAO) and Sternberg Astronomical Institute (SAI) are located;
- the Simeiz Observatory of CrAO, Simeiz, Crimea
- the Special Astrophysical Observatory (SAO), Nizhniy Arkhyz;
- the Moscow Observatory of SAI;
- the Caucasian Mountain Observatory (CMO) of SAI near Kislovodsk

- the Stará Lesná Observatory of the Astronomical Institute of the Slovak Academy of Sciences, Slovakia;
- the Tien-Shan Observatory (TSO) of the Fesenkov Astrophysical Institute near Almaty, Kazakhstan; and
- the Peterhof Observatory of Saint-Petersburg State University.

A list of the observing facilities is given in Table 1.

Table 1. Telescopes and detectors employed for the photometric observations.

Tele-scope code	Location	Aperture [m]	CCD camera	Filters	Scale [arcsec pixel $^{-1}$]	FoV [arcmin]
S60	Stará Lesná	0.6	FLI ML 3041	$UBVR_CI_C$	0.85	14.0
K50	Nauchnyi	0.5	Apogee Alta U8300	$UBVR_CI_C$	1.10	30.5x23.0
K60	Nauchnyi	0.6	Apogee AP-47p	$UBVR_CI_J$	0.7	6.0
M70	Moscow	0.7	Apogee AP-7p	$UBVR_CI_J$	0.64	5.5
M20	Moscow	0.2	Apogee AP-7p	BVR_CI_J	1.22	10.4
S100	Simeiz	1.0	FLI PL09000	$UBVR_CI_C$	0.96	9.8
S60	Simeiz	0.6	VersArray F512	BVR_CI_J	1.37	5.8
A100	TSO	1.0	Apogee Alta U9000	BVR_C	0.38	19.2
N100	SAO	1.0	EEV CCD42-40	$UBVR_CI_C$	0.48	8.3
N600	SAO	6.0	EEV CCD42-40	BVR_CI_C	0.36	6.3
C250	CMO	2.5	EEV CCD44-82	BVR_CI_C	0.15	10.0
P40	Peterhof	0.4	SBIG ST-7XME	BVR_CI_C	2.3	14.3x9.5
K70	Nauchnyi	0.7	SBIG ST-7XME	BVR_CI_C	1.3	8.1x5.4

The standard image reductions and photometry were made using the IRAF¹. The magnitudes of the SN were derived by a PSF-fitting relatively to a sequence of local standard stars.

The CCD image of SN 2014J and local standard stars is presented in Fig. 1.

¹IRAF is distributed by the National Optical Astronomy Observatory, which is operated by AURA under cooperative agreement with the National Science Foundation.

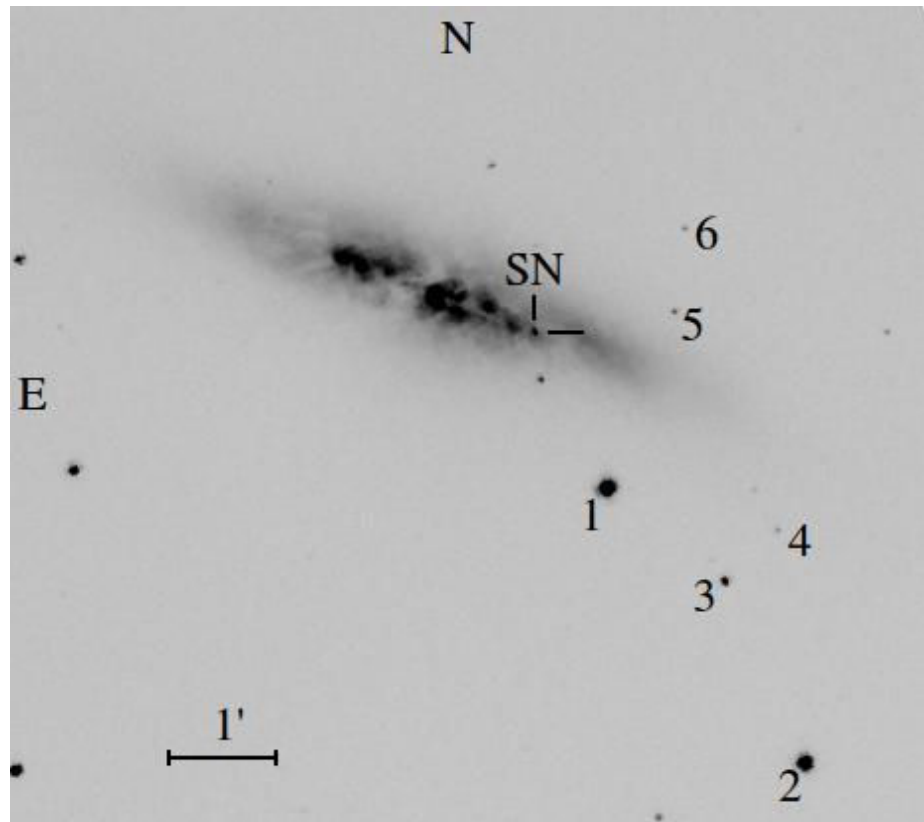


Figure 1. The image of SN 2014J and local standard stars.

The magnitudes of the local standards, calibrated on 15 nights relative to a standard in the field of the nearby galaxy M81 (Richmond et al., 1996), are reported in Table 2.

The surface brightness of the host galaxy at the location of the SN is high, and subtraction of the galaxy background is necessary for accurate photometry. We used the images obtained at the A100 before an SN outburst in 2012, and those taken at the K60 in 2016. These images were transformed, combined and used for galaxy subtraction.

The photometry was transformed to the standard Johnson-Cousins system by means of instrumental colour-terms, determined from observations of standard star clusters.

Our photometry of the SN is presented in Tables 3,4, and 5.

Table 2. $UBVRI$ magnitudes of local standard stars.

Star	U	σ_U	B	σ_B	V	σ_V	R	σ_R	I	σ_I
1	10.84	0.02	10.63	0.01	10.03	0.01	9.70	0.01	9.41	0.01
2	12.15	0.02	11.51	0.01	10.69	0.01	10.23	0.01	9.87	0.01
3	14.29	0.03	14.32	0.01	13.76	0.01	13.43	0.01	13.10	0.01
4			16.31	0.02	16.09	0.02	15.99	0.02	15.87	0.02
5			17.75	0.05	16.31	0.03	15.43	0.02	14.62	0.02
6			17.38	0.04	16.45	0.03	15.93	0.03	15.47	0.03

Table 3.: $UBVRI$ photometry of SN 2014J at 10 telescopes.

JD– 2450000	U	σ_U	B	σ_B	V	σ_V	R	σ_R	I	σ_I	Tel.
6682.13			12.48	0.04	11.18	0.03	10.52	0.03	10.04	0.02	M20
6686.20			12.07	0.03	10.75	0.03	10.24	0.03	9.78	0.02	M20
6687.13			11.98	0.03	10.68	0.02	10.16	0.02	9.73	0.01	M20
6688.17			11.97	0.03	10.65	0.02	10.14	0.02	9.73	0.01	M20
6689.13			11.95	0.02	10.59	0.02	10.11	0.03	9.72	0.02	M20
6691.18	12.70	0.04	11.85	0.02	10.50	0.01	10.05	0.01	9.87	0.02	K50
6692.20	12.77	0.04	11.87	0.02	10.50	0.02	10.06	0.02	9.91	0.02	K50
6693.17	12.77	0.03	11.90	0.02	10.50	0.01	10.08	0.01	9.94	0.02	K50
6694.17	12.71	0.04	11.94	0.02	10.52	0.02	10.08	0.02	9.96	0.02	K50
6694.49	12.86	0.05	12.00	0.02	10.68	0.02	10.11	0.02	10.00	0.03	T60
6695.18			11.99	0.01	10.53	0.02	10.12	0.02	10.00	0.02	K50
6696.16			12.03	0.01	10.54	0.03	10.17	0.02	10.03	0.02	K50
6700.17	13.04	0.07	12.28	0.02	10.71	0.02	10.42	0.02	10.28	0.01	K50
6701.20			12.38	0.01	10.77	0.03	10.52	0.02	10.33	0.02	K50
6702.30	13.44	0.04	12.48	0.01	10.83	0.02	10.60	0.01	10.38	0.02	K50
6702.45	13.51	0.03	12.54	0.01	11.01	0.01	10.57	0.02	10.39	0.03	T60
6706.22	13.99	0.11	12.89	0.01	11.08	0.01	10.77	0.01	10.40	0.02	K50
6707.17	14.07	0.04	12.99	0.01	11.11	0.02	10.81	0.01	10.40	0.03	K50
6708.22			13.19	0.06	11.25	0.03	10.77	0.04			M20
6708.23	14.27	0.07	13.08	0.01	11.15	0.02	10.81	0.02	10.38	0.02	K50
6711.35	14.58	0.06	13.39	0.02	11.28	0.02	10.81	0.02	10.30	0.03	K50
6712.18			13.49	0.05	11.31	0.01	10.81	0.02	10.28	0.02	K50
6712.25	14.83	0.06	13.56	0.02	11.51	0.02	10.76	0.02	10.22	0.02	T60
6714.22			13.79	0.02	11.48	0.02	10.84	0.02	10.14	0.02	M20
6714.40	14.97	0.04	13.71	0.02	11.56	0.02	10.80	0.02	10.13	0.02	T60
6715.18			13.84	0.02	11.51	0.02	10.85	0.02	10.12	0.01	M20
6715.42	15.10	0.03	13.79	0.03	11.62	0.02	10.81	0.01	10.14	0.02	T60
6716.31	15.44	0.04	14.08	0.01	11.59	0.01	10.88	0.01	10.13	0.01	M70
6716.41	15.24	0.07	13.89	0.02	11.67	0.02	10.85	0.03	10.13	0.03	T60
6717.23	15.43	0.03	14.17	0.02	11.63	0.01	10.92	0.02	10.15	0.02	M70
6718.42	15.32	0.03	14.08	0.02	11.74	0.01	10.86	0.02	10.09	0.02	T60

Table 3.: Continued.

JD– 2450000	<i>U</i>	σ_U	<i>B</i>	σ_B	<i>V</i>	σ_V	<i>R</i>	σ_R	<i>I</i>	σ_I	Tel.
6719.31			14.08	0.02	11.64	0.02	10.93	0.02	10.20	0.02	K50
6720.18	15.40	0.05	14.11	0.02	11.68	0.02	10.94	0.01	10.19	0.01	K50
6722.23	15.78	0.06	14.24	0.01	11.79	0.03	11.06	0.01	10.27	0.02	K50
6726.20	15.79	0.10	14.74	0.02	12.16	0.02	11.41	0.01	10.48	0.01	M70
6727.19			14.50	0.03	12.10	0.02	11.41	0.01	10.58	0.02	K50
6730.19			14.63	0.03	12.23	0.02	11.57	0.02	10.78	0.02	K50
6735.20	16.03	0.11	14.71	0.02	12.39	0.03	11.80	0.03	11.07	0.04	K50
6738.21	16.21	0.12	14.83	0.02	12.49	0.01	11.90	0.01	11.21	0.02	K50
6739.20	16.20	0.11	14.79	0.02	12.49	0.02	11.94	0.02	11.27	0.02	K50
6740.23			14.82	0.02	12.54	0.01	11.95	0.01	11.31	0.02	K50
6740.27	16.43	0.07	15.06	0.01	12.67	0.02	12.01	0.01	11.23	0.01	M70
6741.23	16.17	0.12	14.84	0.02	12.57	0.02	12.01	0.01	11.36	0.02	K50
6743.25			15.10	0.01	12.76	0.02	12.13	0.02	11.36	0.01	M70
6745.37	16.13	0.08	14.93	0.04	12.90	0.02	12.16	0.02	11.51	0.04	T60
6746.22			15.15	0.01	12.85	0.02	12.25	0.02	11.51	0.01	M70
6747.25	16.25	0.08	14.97	0.02	12.94	0.01	12.20	0.01	11.56	0.02	K50
6747.27			14.91	0.02	12.76	0.02	12.21	0.02	11.63	0.02	T60
6748.25	16.30	0.08	14.91	0.02	12.78	0.02	12.25	0.02	11.69	0.02	K50
6750.29			15.14	0.03	12.79	0.01	12.33	0.01	11.74	0.02	K50
6751.23	16.54	0.14	14.97	0.02	12.87	0.02	12.34	0.01	11.80	0.02	K50
6751.55	16.32	0.04	15.15	0.02	13.14	0.02	12.39	0.02	11.87	0.02	N100
6755.24			15.00	0.02	12.94	0.02	12.46	0.02	11.96	0.02	K50
6756.25	16.27	0.08			13.14	0.02	12.57	0.02	11.94	0.01	M70
6757.25			15.24	0.01	13.15	0.02	12.59	0.01	11.99	0.01	M70
6758.24	16.54	0.05	15.25	0.01	13.18	0.02	12.63	0.01	12.03	0.01	M70
6758.29	16.60	0.06	15.18	0.02	13.32	0.02	12.59	0.01	12.04	0.02	T60
6761.25	16.90	0.16	15.26	0.02	13.24	0.02	12.70	0.02	12.14	0.02	M70
6762.39			15.17	0.02	13.20	0.04	12.69	0.02			K60
6763.24			15.25	0.02	13.29	0.02	12.73	0.02	12.05	0.02	K60
6768.27	16.70	0.06	15.35	0.02	13.45	0.01	12.93	0.02	12.42	0.02	M70
6771.26			15.31	0.02	13.52	0.02	12.98	0.02			K60
6772.26			15.42	0.01	13.56	0.02	13.05	0.01	12.57	0.01	M70
6774.26			15.25	0.02	13.50	0.02	13.09	0.02	12.69	0.01	K50
6775.30			15.48	0.03	13.63	0.02	13.17	0.03	12.71	0.02	M70
6777.29	17.13	0.17	15.47	0.02	13.68	0.02	13.19	0.02	12.75	0.02	M70
6783.57			15.35	0.02	13.92	0.02	13.38	0.02	13.10	0.03	T60
6785.42			15.34	0.03	13.79	0.04	13.32	0.02			K60
6786.27			15.45	0.02	13.90	0.02	13.42	0.02	12.89	0.03	K60
6786.29			15.40	0.03	13.77	0.03	13.46	0.02	13.13	0.01	K50
6786.30			15.55	0.04	13.95	0.02	13.49	0.01	13.01	0.01	S100
6787.52	17.09	0.14	15.51	0.02	14.00	0.02	13.52	0.01	13.24	0.02	T60
6788.26			15.66	0.03	13.75	0.03	13.37	0.02	13.00	0.03	S100
6788.27			15.43	0.02	13.88	0.02	13.53	0.02	13.22	0.02	K50
6788.39	17.21	0.17	15.53	0.02	14.09	0.02	13.52	0.03	13.21	0.02	T60

Table 3.: Continued.

JD– 2450000	<i>U</i>	σ_U	<i>B</i>	σ_B	<i>V</i>	σ_V	<i>R</i>	σ_R	<i>I</i>	σ_I	Tel.
6789.30	17.26	0.08	15.57	0.02	14.01	0.02	13.57	0.02	13.11	0.02	S100
6790.36			15.62	0.02	14.01	0.02	13.55	0.03	13.12	0.03	S100
6792.25			15.66	0.10	14.04	0.02	13.64	0.02	13.13	0.03	S100
6794.27	17.29	0.19	15.71	0.03	14.18	0.02			13.28	0.01	S100
6795.25			15.66	0.04	14.15	0.02	13.77	0.01	13.29	0.02	S100
6796.29			15.67	0.02	14.16	0.01	13.72	0.01	13.30	0.02	S100
6798.34			15.75	0.01	14.23	0.02	13.80	0.01	13.38	0.02	M70
6799.28			15.59	0.02	14.12	0.02	13.84	0.02	13.49	0.03	K50
6799.34			15.71	0.02	14.24	0.02	13.83	0.02	13.35	0.02	S60
6803.32			15.78	0.03	14.40	0.02	13.89	0.03	13.65	0.03	S100
6803.38	17.51	0.08	15.74	0.02	14.42	0.02	13.95	0.02	13.64	0.03	N100
6805.31			15.77	0.02	14.41	0.02	13.98	0.03	13.65	0.04	K50
6805.40	17.25	0.18	15.71	0.02	14.30	0.02	14.01	0.03	13.66	0.03	S100
6806.29			15.85	0.02	14.42	0.03	14.00	0.02	13.66	0.03	S100
6806.30			15.88	0.03	14.42	0.02	13.98	0.02	13.41	0.02	K60
6807.31			15.76	0.02	14.31	0.03	14.11	0.02	13.70	0.03	K50
6808.29			15.86	0.04	14.51	0.02	14.07	0.03	13.77	0.03	S100
6812.30			15.88	0.05	14.50	0.03	14.21	0.03	13.74	0.03	S60
6818.34			15.95	0.02	14.59	0.01	14.42	0.02	14.01	0.02	K50
6832.29			16.16	0.02	14.90	0.02	14.78	0.02	14.31	0.02	K50
6850.29	18.71	0.09	16.36	0.03	15.32	0.03	15.13	0.02	14.77	0.02	N100
6851.33			16.39	0.03	15.36	0.02	15.13	0.02	14.80	0.02	N100
6852.30			16.45	0.02	15.41	0.02	15.18	0.02	14.83	0.02	N100
6893.26					15.99	0.05	16.06	0.11			K50
6896.31			17.08	0.04	16.18	0.03	15.99	0.03	15.03	0.03	K60
6897.24			17.10	0.03	16.20	0.03	16.01	0.03	15.08	0.02	K60
6899.27			17.21	0.03	16.19	0.02	16.05	0.03	15.03	0.02	K60
6900.24			17.07	0.07	16.17	0.03	16.06	0.03	15.00	0.03	K60
6901.24			17.12	0.05	16.25	0.04	15.99	0.03	15.11	0.05	K60
6902.24			17.07	0.04	16.21	0.03	16.03	0.03	15.17	0.04	K60
6904.23			17.12	0.08	16.21	0.02	16.05	0.04	15.24	0.05	K60
6905.23					16.29	0.04	16.14	0.03	15.36	0.08	K60
6906.22					16.25	0.04	16.11	0.03	15.35	0.06	K60
6908.23			17.15	0.06	16.34	0.04	16.20	0.03	15.33	0.05	K60
6916.47			17.34	0.05	16.51	0.05	16.36	0.04	15.55	0.07	K60
6919.45			17.60	0.07	16.62	0.05	16.44	0.04	15.60	0.07	K60
6941.43			17.86	0.09	16.90	0.03	16.79	0.04	15.79	0.05	K60
6959.61					17.11	0.05	17.05	0.04	16.23	0.05	N100
6967.38			17.92	0.08	17.22	0.04	17.15	0.04	16.18	0.05	K60
6969.44			18.14	0.08	17.30	0.03	17.15	0.05	16.18	0.09	K60
6973.47			18.18	0.06	17.31	0.04	17.22	0.04	16.14	0.05	K60
6974.60			18.16	0.06	17.31	0.03	17.27	0.03	16.49	0.04	N100
6983.55			18.33	0.04	17.46	0.04	17.40	0.04	16.51	0.04	N100
7040.56			18.99	0.12	17.95	0.08	17.88	0.07			N600

Table 3.: Continued.

JD– 2450000	<i>U</i>	σ_U	<i>B</i>	σ_B	<i>V</i>	σ_V	<i>R</i>	σ_R	<i>I</i>	σ_I	Tel.
7071.40					18.44	0.12					S100
7073.14			19.54	0.07	18.49	0.06	18.26	0.09	17.38	0.06	C250
7074.52					18.49	0.05					S100
7078.30									17.17	0.10	S100
7106.27							18.42	0.15			K60

Table 4.: *BVRI* photometry of SN2014J at the P40 and K70 telescopes.

JD– 2456000	<i>B</i>	σ_B	<i>V</i>	σ_V	<i>R</i>	σ_R	<i>I</i>	σ_I	Tel.
681.26					10.73	0.04			P40
681.27	12.75	0.04	11.39	0.04	10.72	0.04	10.32	0.02	P40
685.32	12.11	0.01	10.84	0.02	10.25	0.02	9.89	0.01	P40
686.28	12.07	0.02	10.77	0.02	10.17	0.02	9.87	0.01	P40
687.25	12.01	0.02	10.73	0.01	10.16	0.02	9.85	0.01	P40
688.38	11.98	0.01	10.68	0.01	10.13	0.01	9.84	0.01	P40
693.36	12.00	0.01	10.61	0.01	10.12	0.02	9.98	0.02	K70
694.39	12.05	0.05	10.63	0.02	10.13	0.03	10.01	0.03	K70
695.29	12.07	0.02	10.65	0.01	10.14	0.02	10.06	0.01	P40
713.32	13.61	0.04	11.53	0.03	10.84	0.01	10.27	0.02	P40
715.47	13.85	0.03	11.60	0.02	10.88	0.02	10.20	0.03	P40
716.49					10.90	0.01			P40
717.26	14.03	0.02	11.71	0.03	10.91	0.01	10.21	0.02	P40
724.32	14.54	0.02	12.09	0.01	11.26	0.03	10.38	0.02	P40
726.42					11.42	0.02	10.55	0.01	P40
728.38	14.61	0.06	12.32	0.03	11.54	0.02	10.70	0.02	P40
729.32	14.73	0.02	12.37	0.01	11.59	0.01	10.74	0.02	P40
730.39	14.74	0.02	12.43	0.03	11.65	0.02	10.82	0.03	P40
731.38	14.77	0.03	12.47	0.02	11.70	0.02	10.87	0.03	P40
734.24			12.55	0.02	11.82	0.02			P40
736.35	14.86	0.03	12.63	0.01	11.88	0.01	11.13	0.01	P40
738.27	14.98	0.02	12.70	0.03	11.97	0.02	11.25	0.03	P40
739.25	14.95	0.02	12.72	0.02	11.98	0.02	11.28	0.03	P40
743.38	15.06	0.04	12.79	0.03	12.12	0.04	11.46	0.02	P40
744.29	14.95	0.05	12.76	0.05	12.10	0.05	11.45	0.03	P40
744.30	14.99	0.03	12.90	0.02	12.15	0.01	11.44	0.03	K70
745.52	15.09	0.04	12.87	0.03	12.19	0.03	11.56	0.02	P40
746.42	15.08	0.03	12.91	0.02	12.22	0.02	11.61	0.01	P40
752.35	15.17	0.03	13.11	0.02	12.40	0.03	11.87	0.04	P40
753.33					12.44	0.03			P40
755.35	15.31	0.05	13.25	0.04	12.46	0.06	12.01	0.04	P40

Table 4.: Continued.

JD – 2456000	<i>B</i>	σ_B	<i>V</i>	σ_V	<i>R</i>	σ_R	<i>I</i>	σ_I	Tel.
756.32	15.16	0.04	13.17	0.04	12.57	0.01	12.05	0.02	P40
757.30	15.29	0.04	13.25	0.01	12.59	0.02	12.10	0.02	P40
758.42	15.24	0.04	13.25	0.01	12.62	0.02	12.14	0.02	P40
760.31	15.14	0.03	13.31	0.01	12.65	0.03	12.19	0.02	P40
764.39	15.28	0.05	13.38	0.04	12.78	0.03	12.39	0.02	P40
765.32	15.22	0.05	13.45	0.02	12.84	0.02	12.40	0.03	P40
766.44	15.27	0.03	13.50	0.02	12.86	0.03	12.41	0.03	P40
767.37	15.23	0.07	13.46	0.04	12.89	0.01	12.48	0.02	P40
768.34	15.28	0.04	13.51	0.02	12.84	0.06	12.47	0.04	P40
769.30	15.22	0.05	13.49	0.03	12.92	0.03	12.54	0.02	K70
770.27	15.24	0.05	13.53	0.03	12.95	0.03	12.58	0.02	K70
770.34	15.27	0.06	13.56	0.03	12.97	0.02	12.58	0.02	P40
771.34	15.21	0.06	13.59	0.04	13.00	0.03	12.57	0.02	K70
772.32	15.33	0.06			13.03	0.03	12.69	0.02	K70
773.28	15.22	0.04	13.65	0.03	13.04	0.03	12.71	0.02	K70
773.35	15.38	0.04	13.63	0.03	13.07	0.03	12.74	0.04	P40
775.32	15.33	0.03	13.68	0.02	13.14	0.02	12.81	0.02	K70
780.39	15.36	0.08	13.83	0.05	13.25	0.04	12.95	0.05	P40
780.47	15.42	0.01	13.83	0.02	13.27	0.02	12.98	0.02	K70

Spectroscopic observations were carried out at the 2.6-m Shajn telescope of CrAO on 5 dates from February 4 until June 29, 2014. The spectrograph SPEM provided the wavelength range of 3300–7550 Å with a dispersion of 2Åpixel $^{-1}$. The spectra were bias and flat-field corrected, extracted and wavelength calibrated with the SPERED code developed by S.I. Sergeev at the CrAO. The spectrophotometric standard HR3894 was used for flux calibrated spectra.

At SAO spectroscopic observations were obtained at the 1-meter telescope with a spectrograph UAGS, which provided the wavelength range of 3507–7885 Å with a dispersion of 2.2 Åpixel $^{-1}$, and at the 6-meter telescope with a SCORPIO focal reducer and grisms VPHG550G and VPHG1200G. The grism VPHG1200G provided the wavelength range of 4044–5858 Å with a dispersion of 0.88 Åpixel $^{-1}$, while the grism VPHG550G yielded the range of 3670–7906 Å and a dispersion of 2.3 Åpixel $^{-1}$.

The spectra were bias and flat-field corrected, extracted and wavelength calibrated in ESO/MIDAS. The spectrophotometric standard AGK+81°266 was used for flux calibrated spectra.

Table 5. *BVR* observations of SN2014J at the A100 telescope.

JD– 2450000	<i>B</i>	σ_B	<i>V</i>	σ_V	<i>R</i>	σ_R
6697.37	12.11	0.02	10.59	0.01	10.10	0.01
6697.51	12.11	0.02	10.60	0.01	10.11	0.01
6698.29	12.23	0.01	10.69	0.01	10.23	0.01
6698.42	12.24	0.01	10.69	0.01	10.23	0.01
6705.49	12.88	0.01	11.13	0.02	10.68	0.02
6715.41	13.93	0.02	11.52	0.05	10.82	0.04
6717.10	14.08	0.02	11.61	0.02	10.84	0.04
6719.07	14.23	0.02	11.69	0.02	10.90	0.02
6720.06	14.31	0.03	11.73	0.03	10.93	0.04
6721.08	14.40	0.02	11.73	0.09	11.05	0.01
6722.07	14.44	0.02	11.85	0.04	11.00	0.05
6727.10	14.73	0.01	12.22	0.01	11.60	0.01
6728.07	14.75	0.01	12.25	0.01	11.48	0.01
6729.07	14.79	0.01	12.32	0.01	11.61	0.01
6748.09	15.06	0.01	12.90	0.01	12.27	0.01
6749.08	15.08	0.02	12.89	0.03	12.31	0.01
6751.19	15.16	0.03	12.96	0.03	12.36	0.01
6756.11	15.15	0.01	13.11	0.01	12.51	0.01
6757.21	15.13	0.01	13.14	0.01	12.56	0.01
6758.18	15.11	0.03	13.16	0.02	12.58	0.02
6759.23	15.15	0.05	13.12	0.04	12.58	0.01
6780.26	15.44	0.04	13.78	0.03	13.26	0.03
6782.20	15.45	0.04	13.80	0.03	13.29	0.03
6787.16	15.52	0.04	13.92	0.03	13.44	0.03
6789.14	15.59	0.04	14.01	0.03	13.54	0.03
6791.15	15.59	0.04	14.05	0.03	13.58	0.03
6792.21	15.61	0.04	14.06	0.03	13.58	0.03
6795.31	15.65	0.04	14.17	0.03	13.72	0.02
6801.16	15.74	0.04	14.32	0.02	13.88	0.02
6802.17	15.76	0.04	14.35	0.03	13.92	0.03
6809.14	15.86	0.04	14.50	0.03	14.10	0.02
6837.15			15.09	0.03	14.78	0.04
7001.42	18.51	0.06	17.58	0.05	17.59	0.05

3. Light and colour curves

The complete light curves of SN 2014J are presented in Fig. 2, and the curves around the maximum are shown in Fig. 3.

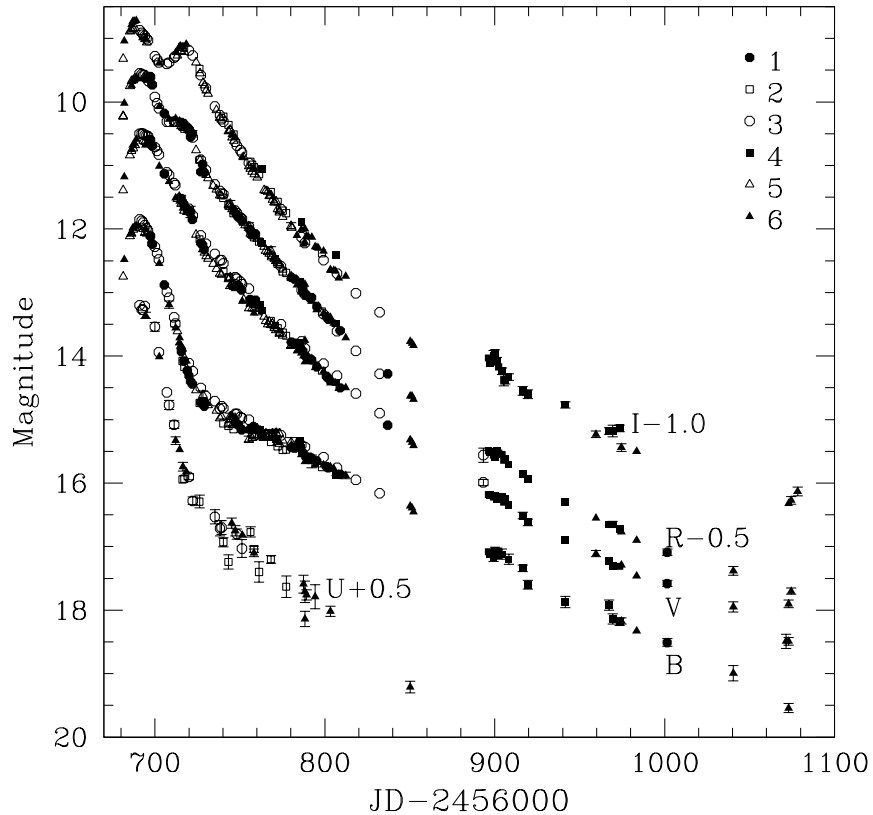


Figure 2. The light curves of SN 2014J in the *UBVRI* bands. The curves are shifted vertically for clarity, the amount of shift is indicated on the plot. The error bars are plotted only when they exceed the size of a symbol. The shape of the symbols corresponds to the instruments used: 1 - A100, 2 - M70, 3 - K50, 4 - K60, 5 - P40 and K70, and 6 - other telescopes.

The results for all the telescopes are in a fairly good agreement, but some systematic differences can be noted. At phase near the maximum the differences in the *I*-band magnitudes between M20 and P40 are evident, and soon after the maximum the *V*-band magnitudes from P40 and M20 are ~ 0.1 mag lower than

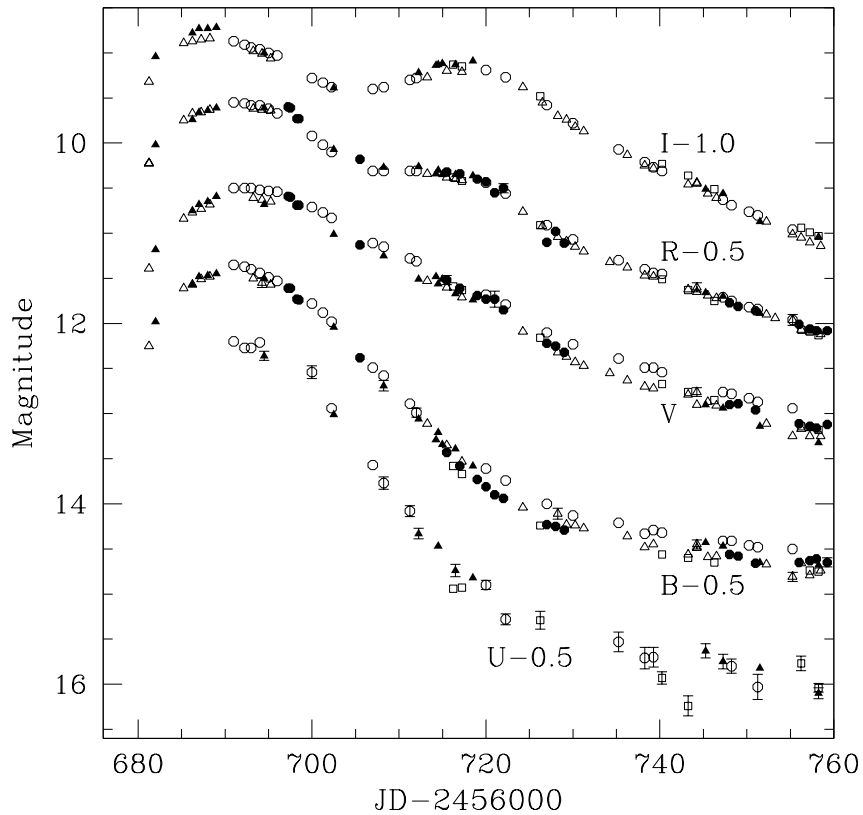


Figure 3. The light curves of SN 2014J near the maximum light.

those from K50. At the phase ~ 30 days past the maximum the difference in the B -magnitudes becomes evident, estimates from K50 are about 0.2 mag higher than those from other sources.

The light curves from five major data sets (Amanullah et al. (2014), Kawabata et al. (2014), Foley et al. (2014), Marion et al. (2015), and Srivastav et al. (2016)) are compared in Fig. 4. The large differences of the B magnitudes at phases 30–60 days are revealed. The difference between brightest (Foley et al., 2014) and faintest (Kawabata et al., 2014) estimates amounts to 0.5 mag. Our magnitudes from K50 are closer to the data from Foley et al. (2014), while data from other telescopes are in good agreement with the results by Srivastav et al. (2016).

The agreement between various sets of the U -band magnitudes is very poor.

While there is reasonable agreement between data from Srivastav et al. (2016) and Marion et al. (2015), our data and magnitudes from Amanullah et al. (2014) are ~ 0.3 mag fainter at all phases, and the results from the Swift satellite² are further 0.5 mag fainter.

The agreement of the V , R and I magnitudes is much better, with the maximum difference not exceeding 0.2 mag.

We conclude that photometry of such a red object on bright background faces significant problems. It is clear that the transformation of instrumental magnitudes to the standard Johnson-Cousins system using linear colour terms is not accurate in this case. Unfortunately, we have no possibility to apply the S-correction method (Stritzinger et al., 2002), and have to take the average values as more reliable.

We fitted the photometric data near the maximum with cubic splines and determined the dates and magnitudes of maximum light and the decline parameters Δm_{15} in different bands. The calculations were carried out for our data and for the combination of our data with the results from the authors listed above. The results are presented in Table 6. The differences between the estimates of maximum magnitudes are very small, but there are some distinctions in determination of dates of maximum and Δm_{15} .

Table 6. Dates and magnitudes of maximum light (for the I -band also for the secondary maximum) and the decline rate parameters in different passbands. The results for our data are reported at the upper part, and those for the combination of our photometry with the data from other authors are at the lower part.

Band	JD–2456000	mag	Δm_{15}
B	690.6 ± 0.7	11.91 ± 0.05	0.96 ± 0.05
V	692.4 ± 0.6	10.53 ± 0.04	0.64 ± 0.04
R	692.8 ± 0.5	10.06 ± 0.04	0.77 ± 0.05
I	688.4 ± 0.9	9.75 ± 0.08	0.65 ± 0.10
I_{sec}	717.2 ± 0.6	10.15 ± 0.04	
U	687.4 ± 1.1	12.55 ± 0.08	0.91 ± 0.2
B	691.6 ± 0.8	11.93 ± 0.05	1.10 ± 0.05
V	692.4 ± 0.5	10.55 ± 0.03	0.70 ± 0.05
R	691.2 ± 0.5	10.09 ± 0.04	0.70 ± 0.05
I	688.3 ± 0.9	9.80 ± 0.08	0.57 ± 0.10
I_{sec}	717.3 ± 0.5	10.15 ± 0.04	

As our observations continued for more than 400 days after the maximum, it is possible to determine the rates of decline on the exponential tail, which started at about 100 days after the maximum light.

²http://people.physics.tamu.edu/pbrown/SwiftSN/swift_sn.html

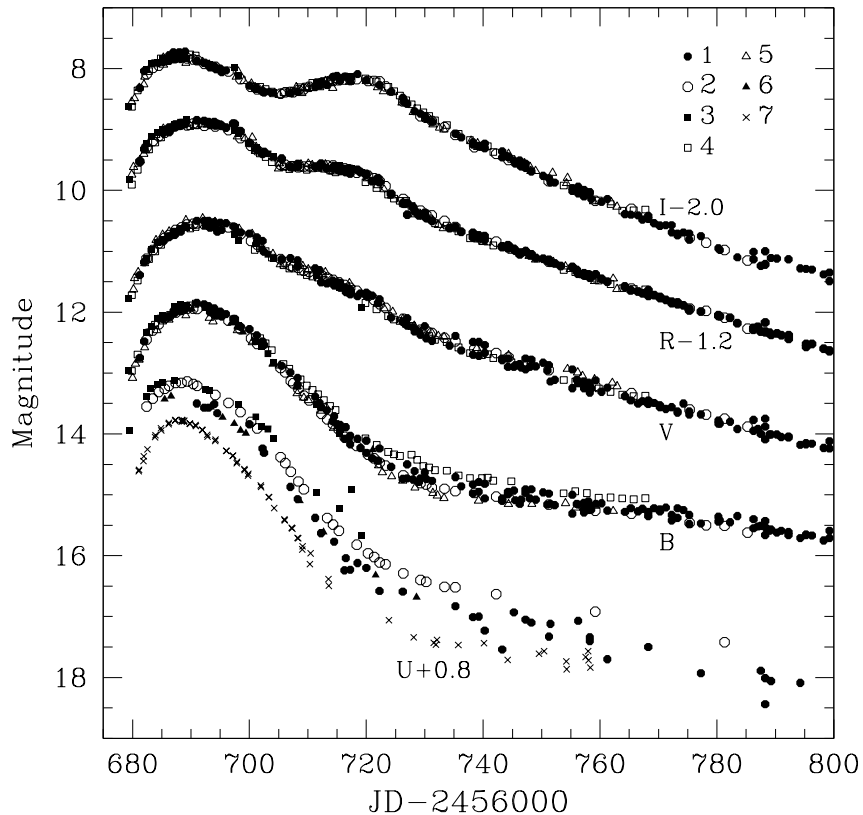


Figure 4. The light curves of SN 2014J from different data sets: 1 - this work, 2 - Srivastav et al. (2016), 3 - Marion et al. (2015), 4 - Foley et al. (2014), 5 - Kawabata et al. (2014), 6 - Amanullah et al. (2014), and 7 - Swift.

The decline rates in magnitudes per day on the exponential tail in the *BVRI*-bands, determined by linear least-square fitting, are 0.0140 ± 0.0003 , 0.0142 ± 0.0002 , 0.0139 ± 0.0002 , and 0.0127 ± 0.0002 , respectively. The decline rates in the *B*, *V* and *R* bands are virtually the same, while the *I*-band decline is slower.

The comparison of light curves for SN 2014J and SNe Ia with a similar value of Δm_{15} is presented in Fig. 5. The light curves in the *U*, *V* and *R* bands are practically identical for all SNe. The most evident difference is for the *B*-band at a phase interval of 30–50 days. At that stage there is a pronounced protrusion on the *B*-band light curve of SN 2014J, SNe 2002bo (Benetti et al., 2004) and 2006X

(Wang et al., 2008) show similar behaviour. The light curves of SNe 2003du (Stanishev et al., 2007), 2005cf (Wang et al., 2009b) and 2011fe (Tsvetkov et al., 2013) are linear after the bend from fast decay to the tail, and the difference between these SNe and SN 2014J is evident.

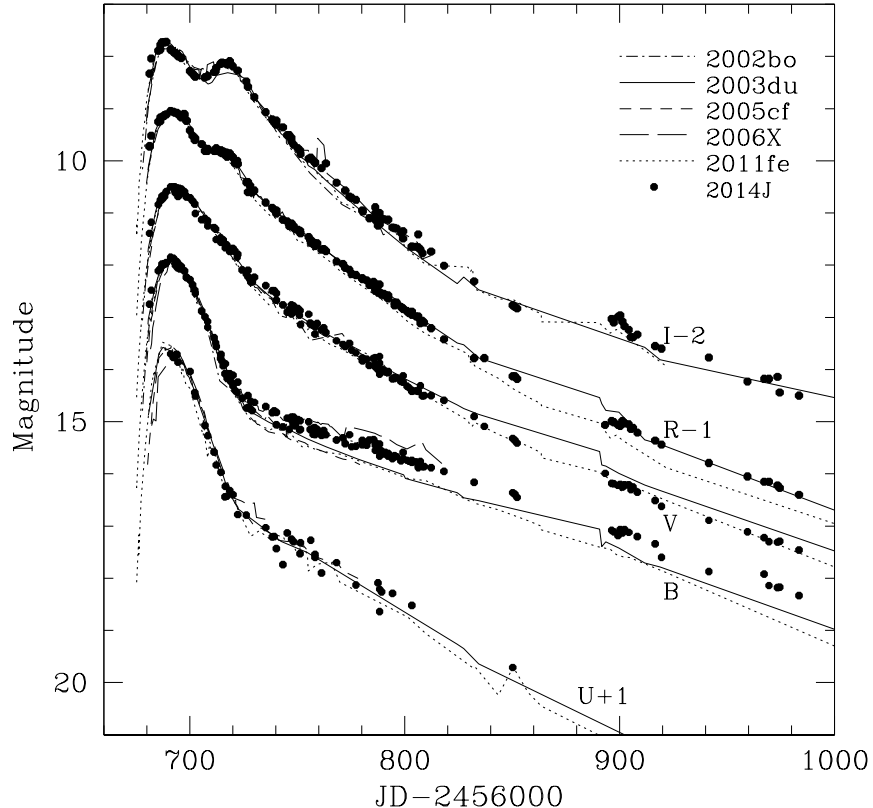


Figure 5. Comparison of the light curves of SN 2014J with those for 5 SNe Ia with nearly the same Δm_{15} .

The colour curves for SN 2014J are presented in Fig. 6. The colour evolution is typical for SNe Ia, this is confirmed by comparison with the colour curves for SNe 2002bo, 2003du, 2005cf, 2006X and 2011fe. The colour curves of these SNe are in general agreement with the curves for SN 2014J, although some differences are revealed. The $(B - V)$ colour of SN 2014J is significantly bluer at phase > 100 days than for SNe 2011fe and 2003du, while the $(V - R)$ colour is redder.

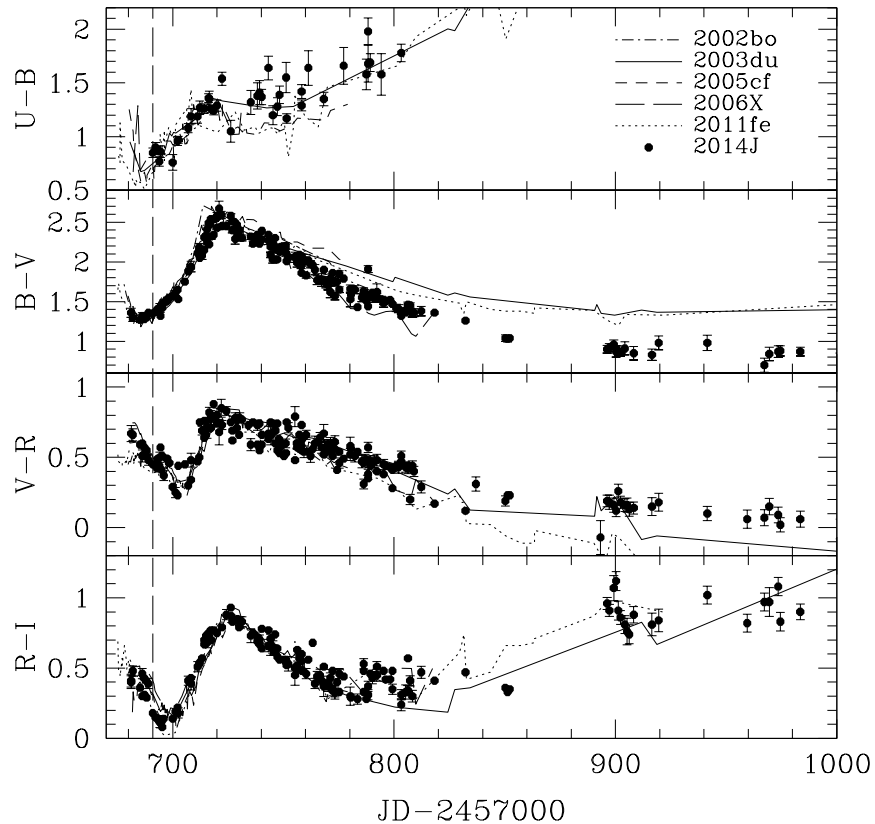


Figure 6. The colour curves of SN 2014J and comparison with those for 5 SNe Ia with nearly the same Δm_{15} . The time of B -band maximum is shown by a vertical dashed line.

The amount of shift applied to match the curves can be considered as an estimate of the colour excess of SN 2014J. We adopted the following colour excesses $E(B - V)$ for the SNe 2002bo, 2003du, 2005cf, 2006X, and 2011fe: 0.43, 0.01, 0.09, 1.26, and 0.01 mag, respectively, from the works cited earlier.

We obtained the following estimates: $E(U - B) = 1.07 \pm 0.10$, $E(B - V) = 1.38 \pm 0.04$, $E(V - R) = 0.44 \pm 0.04$, and $E(R - I) = 0.56 \pm 0.05$ mag.

The $(B - V)$ colour curve is also compared with the "Lira-Phillips" relation (Phillips et al., 1999), showing the time dependence of $(B - V)$ in the phase interval 30–90 days after the maximum for SNe Ia that suffered no extinction. This method yields $E(B - V) = 1.35 \pm 0.02$ mag, in good agreement with the

previous estimate. We adopt the mean value $E(B - V) = 1.36 \pm 0.03$ mag as most probable.

The colour excess due to the galactic extinction is $E(B - V)_{gal} = 0.14$ mag according to Schlafly & Finkbeiner (2011), so the colour excess in the host galaxy is $E(B - V)_{host} = 1.22$. If we assume the distance modulus for M82 $\mu = 27.73$ (Karachentsev & Kashibadze, 2006), then the absolute magnitudes, corrected for the galactic extinction, are -16.37 and -17.61 mag in the B and V bands, respectively.

Our value of $\Delta m_{15}(B) = 0.96$ is the same as determined by Srivastav et al. (2016), so we conclude that the true value of this parameter, corrected for the colour excess, is $\Delta m_{15}(B)_{true} = 1.08$.

According to the calibration of the Pskovskiy-Phillips relation by Prieto et al. (2006), the mean absolute magnitudes for SN Ia with $\Delta m_{15}(B) = 1.08$ are $M_B = -19.33$ and $M_V = -19.26$ mag.

We can calculate the most probable values of extinction in the host galaxy $A_B = 2.96$ and $A_V = 1.65$ mag. Using our estimate $E(B - V)_{host} = 1.22$ mag, we obtain the ratio of total-to-selective extinction $R_V = A_V/E(B - V) = 1.35$, in good agreement with the results of Foley et al. (2014).

This number is much smaller than the typical galactic value of 3.1, but close to the values found for another heavily reddened type Ia SNe (Wang et al., 2008).

4. Search for microvariability

Typical photometric monitoring of SNe consists of a single or few observations per night, so the short-timescale and low-amplitude variability remains poorly studied. Bonanos & Boumis (2016) reported evidence for microvariability in the optical light curve of SN 2014J. They obtained high-precision photometry in the B, V bands with a cadence of 2 min for about 8 hours per night during 4 consecutive nights at the phase ~ 16 days past maximum, and reported statistically significant detection of microvariability at the level of 0.02–0.05 mag with characteristic time 15–60 min on all nights.

We carried out photometric monitoring of SN 2014J at the A100 telescope during 6 nights from February 8 until March 3, 2014. Series of images in the B, V, R bands were obtained with exposure times of 60, 40, and 30 sec, the time lapse between consequent exposures in one filter was 3.5 min. The longest monitoring period was on the night of February 8/9, when it lasted for 7 hours, on the night February 9/10 observations lasted 5.8 hours and on the other nights monitoring continued for 3–1.3 hours.

We performed aperture photometry of SN relative to local standard stars 1 and 2 (S1, S2). Unfortunately, star 1 was overexposed on many frames in the V, R bands, and star 2 was often out of the field of view.

Typical photometric errors are 0.001–0.002 mag for the stars S1, S2 in all bands; for the SN the errors are about 0.002–0.003 mag in the V, R bands, for the B band they are 0.003–0.004 mag for the first nights in February, but increase to 0.015–0.02 mag for the nights in March.

Fig. 7 shows the data for the night February 8/9.

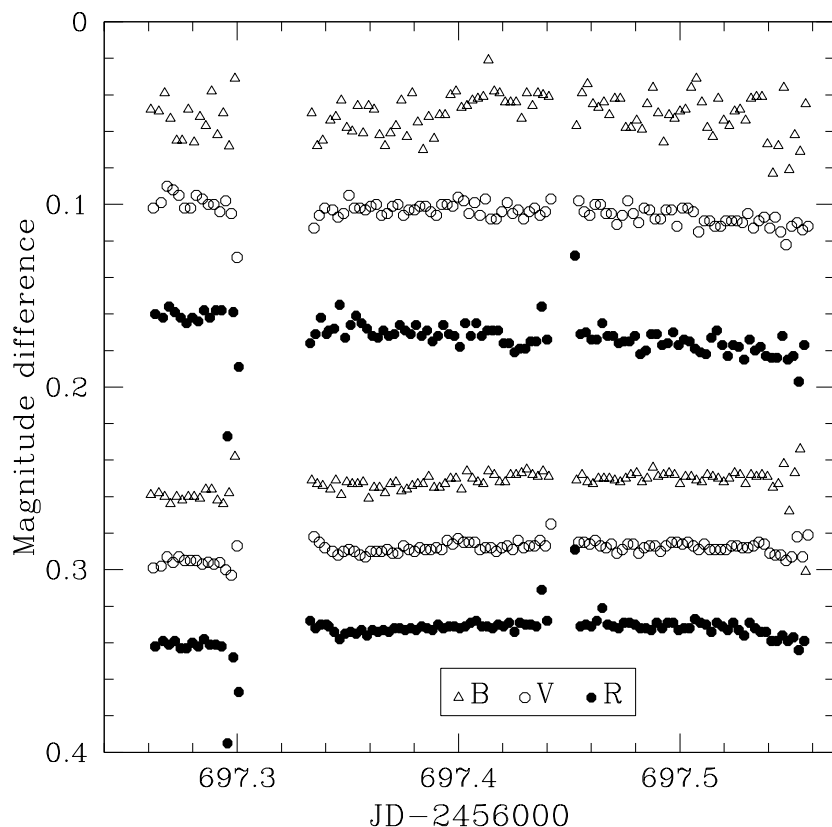


Figure 7. Results of monitoring of SN 2014J for the night February 8/9. 3 upper rows: magnitude differences $\Delta(\text{SN}-\text{S}1)$, 3 lower rows: magnitude differences $\Delta(\text{S}2-\text{S}1)$. The data were shifted vertically for clarity.

On the night February 8/9 the observations were interrupted by clouds, this is the reason for breaks in the monitoring and large magnitude deviations near the breaks.

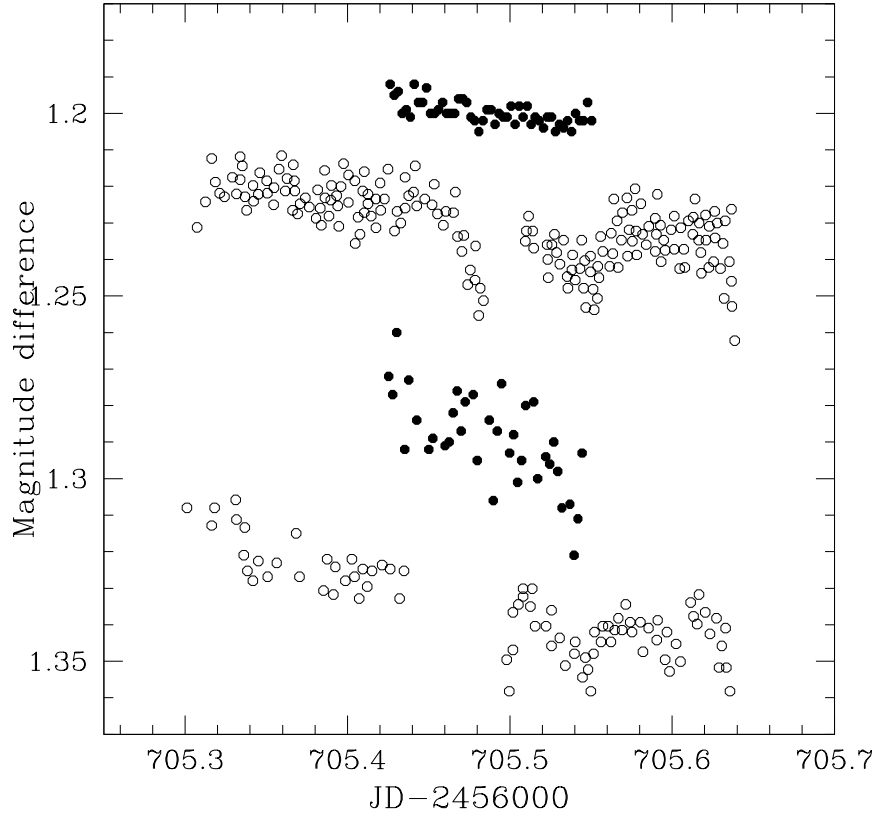


Figure 8. Results of monitoring of SN 2014J for the night February 16/17. Dots show our data, circles present the results by Bonanos & Boumis (2016). The magnitude differences $\Delta(S1-SN)$ are shown for the V -band in two upper rows, and for the B -band in two lower rows. The data were shifted vertically for clarity.

The differences of instrumental magnitudes $\Delta(S1-SN)$, $\Delta(S2-SN)$ were approximated by a first-order polynomial, and the regression coefficients and the standard deviations σ were calculated. The same procedure was applied to the magnitude differences of stars S1 and S2.

The minimal value of standard deviations $\sigma(S1-SN)$ and $\sigma(S2-SN)$ is 0.009 mag in the B band and 0.003 mag in the V, R -bands. On the nights when both stars 1 and 2 were measured, $\sigma(S1-S2)$ was never significantly less than $\sigma(S1-SN)$ and $\sigma(S2-SN)$ for the V - and R -bands. Besides, no quasiperiodical SN brightness variations can be noticed on the plots of $\Delta(S1-SN)$ and $\Delta(S2-SN)$ versus time.

On the night February 16/17 monitoring was carried out at A100 and by Bonanos & Boumis (2016). Fig. 8 shows the comparison of results. Our observations do not confirm the dimming of SN in the V -band at JD 2456705.48 and 2456705.54, noticed by Bonanos & Boumis (2016).

We conclude that our observations do not confirm the existence of microvariability of SN 2014J with the amplitude and characteristic time reported by Bonanos & Boumis (2016).

5. Spectra

The spectra of SN 2014J obtained at the 2.6-meter telescope of CrAO are shown in Fig. 9, and those collected at the N600 and N100 telescopes are presented in Fig. 10.

The spectral evolution is typical for SN Ia, and the results are in good agreement with the data from Srivastav et al. (2016), Kawabata et al. (2014), Marion et al. (2015), and Bikmaev et al. (2015). The expansion velocities from the absorption features of the early spectra, obtained at the 2.6-meter telescope, were calculated by Tsvetkov et al. (2014). We used the radial velocity of the galaxy M82 $v_{hel}=203$ km s $^{-1}$ to correct the observed shift of the lines, but Bikmaev et al. (2015) took into account the rotation of the galaxy and obtained a smaller radial velocity, $v_{hel}=111$ km s $^{-1}$, for the site of the SN. Using this value and measuring also the spectrum obtained at SAO, we calculate the following expansion velocities for the SiII λ 6355 line: 11700, 11510, and 10750 km s $^{-1}$ for phases 2, 5 and 31 days after the maximum, respectively. These results are in good agreement with the data from Marion et al. (2015), Kawabata et al. (2014), and Srivastav et al. (2016), and they confirm that SN 2014J is located at the border of the Normal Velocity and High Velocity groups of SNe Ia (Wang et al., 2009a), in the Low Velocity Gradient subclass (Benetti et al., 2005).

The nebular spectra at phase > 100 days are dominated by emission features of [FeIII] λ 4071, [FeII] λ 5159,5261 and NaI/[CoIII] features near 5900Å. We measured the velocity of the [FeIII] λ 4071 emission feature and found the following values: -3000 , -2280 , -1630 , and -110 km s $^{-1}$ for phases 96, 124, 147, and 350 days after the maximum, respectively. We confirm the evolution of the redshift for this line, but our velocities are smaller than those obtained by Srivastav et al. (2016).

The strong interstellar NaI line is a characteristic feature of the spectra, with equivalent width 5.8 Å. The relation $E(B-V) = 0.16EW(\text{NaI})$ (Turatto et al., 2003) gives $E(B-V) = 0.93$ mag. We consider this reasonable agreement with the value of $E(B-V)$ determined from the comparison of colour curves, taking into account the low correlation degree of this relation (Poznanski et al., 2011).

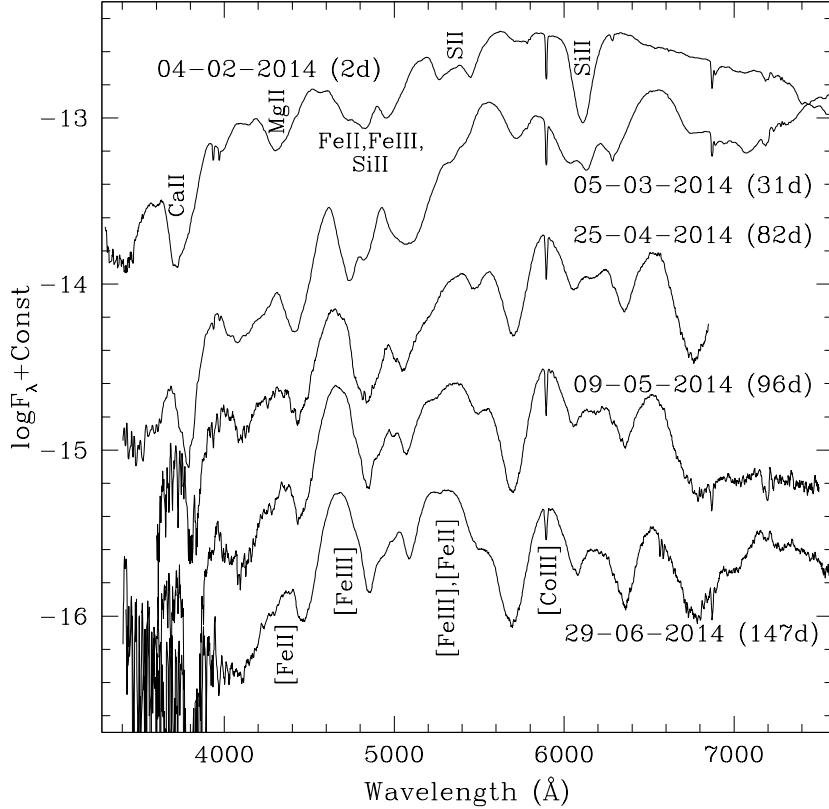


Figure 9. Spectra of SN 2014J collected at the 2.6-m Shajn telescope of CrAO. The date and phase past the B -band maximum are plotted near each spectrum.

6. Conclusions

We present the light and colour curves of SN 2014J spanning the phase interval from -8 to $+416$ days since the B -band maximum, and 9 spectra covering the period 2–350 days after the maximum. The light and colour curves are typical for SNe Ia, with a normal decline rate $\Delta m_{15}(B) = 1.08$. The interstellar extinction in the parent galaxy is very high, with $E(B-V)_{host} = 1.22$ and $R_V = 1.36$. The comparison of photometric data sets from 5 works reveals significant differences, especially for the U and B -bands, and for the period when the SN reached its maximum red colour.

The continuous photometric monitoring of SN 2014J on 6 nights does not reveal microvariability with the amplitude and characteristic time reported by

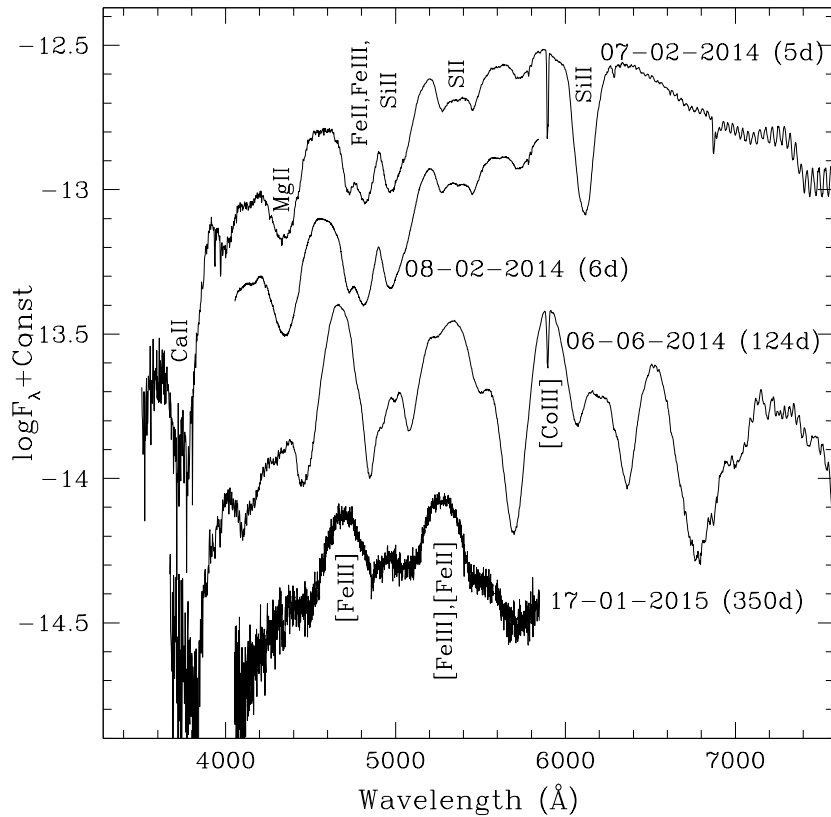


Figure 10. Spectra of SN 2014J acquired at the N100 (07-02-2014) and N600 (3 other spectra) telescopes of SAO.

Bonanos & Boumis (2016).

The spectral features are the same as for normal SNe Ia, the velocity evolution places SN 2014J at the border of the Normal Velocity and High Velocity groups, in the Low Velocity Gradient subclass. At the nebular stage we reveal the blue shift of $[\text{FeIII}]\lambda 4701$ emission, which decreases with time.

Acknowledgements

The work of D.Tsvetkov was partly supported by the Russian Science Foundation Grant No. 16-12-10519.

The work of S.Shugarov was partly supported by Grants VEGA 2/0008/17 and APVV-15-0458.

This study was partly supported by the scholarship of the Slovak Academic Information Agency and by the Russian Science Foundation Grant No. 14-12-00146.

This study was also supported by the Committee on Science of the Ministry of Education and Science of the Republic of Kazakhstan (project no. BR05236322).

The authors are grateful to Savchenko S.S., Larionov V.M., Grishina T.S., Morozova D.A., Kopatskaya E.N., Larionova L.V., Borman G.A., who carried out some of the observations.

References

- Amanullah, R., Goobar, A., Johansson, J., et al., The Peculiar Extinction Law of SN 2014J Measured with the Hubble Space Telescope. 2014, *Astrophys. J., Lett.*, **788**, L21, DOI: 10.1088/2041-8205/788/2/L21
- Ashall, C., Mazzali, P., Bersier, D., et al., Photometric and spectroscopic observations, and abundance tomography modelling of the Type Ia supernova SN 2014J located in M82. 2014, *Mon. Not. R. Astron. Soc.*, **445**, 4427, DOI: 10.1093/mnras/stu1995
- Astier, P., Guy, J., Regnault, N., et al., The Supernova Legacy Survey: measurement of Ω_M , Ω and w from the first year data set. 2006, *Astron. Astrophys.*, **447**, 31, DOI: 10.1051/0004-6361:20054185
- Benetti, S., Cappellaro, E., Mazzali, P. A., et al., The Diversity of Type Ia Supernovae: Evidence for Systematics? 2005, *Astrophys. J.*, **623**, 1011, DOI: 10.1086/428608
- Benetti, S., Meikle, P., Stehle, M., et al., Supernova 2002bo: inadequacy of the single parameter description. 2004, *Mon. Not. R. Astron. Soc.*, **348**, 261, DOI: 10.1111/j.1365-2966.2004.07357.x
- Bikmaev, I. F., Chugai, N. N., Sunyaev, R. A., et al., Type Ia supernovae 2014J and 2011fe at the nebular phase. 2015, *Astronomy Letters*, **41**, 785, DOI: 10.1134/S1063773715120014
- Bonanos, A. Z. & Boumis, P., Evidence for rapid variability in the optical light curve of the Type Ia SN 2014J. 2016, *Astron. Astrophys.*, **585**, A19, DOI: 10.1051/0004-6361/201425412
- Denisenko, D., Gorbovskoy, E., Lipunov, V., et al., MASTER-Net Prediscovery and Follow-up Observations of SN 2014J in M82. 2014, *The Astronomer's Telegram*, **5795**
- Foley, R. J., Fox, O. D., McCully, C., et al., Extensive HST ultraviolet spectra and multiwavelength observations of SN 2014J in M82 indicate reddening and

- circumstellar scattering by typical dust. 2014, *Mon. Not. R. Astron. Soc.*, **443**, 2887, DOI: 10.1093/mnras/stu1378
- Gerke, J. R., Kochanek, C. S., & Stanek, K. Z., LBT R-band Variability Limit for the Progenitor of SN 2014J. 2014, *The Astronomer's Telegram*, **5808**
- Goobar, A., Johansson, J., Amanullah, R., et al., The Rise of SN 2014J in the Nearby Galaxy M82. 2014, *Astrophys. J., Lett.*, **784**, L12, DOI: 10.1088/2041-8205/784/1/L12
- Goobar, A., Kromer, M., Siverd, R., et al., Constraints on the Origin of the First Light from SN 2014J. 2015, *Astrophys. J.*, **799**, 106, DOI: 10.1088/0004-637X/799/1/106
- Itagaki, K., Kaneda, H., Yamaoka, H., et al., Supernova 2014J in M82 = Psn J09554214+6940260. 2014, *Central Bureau Electronic Telegrams*, **3792**
- Karachentsev, I. D. & Kashibadze, O. G., Masses of the local group and of the M81 group estimated from distortions in the local velocity field. 2006, *Astrophysics*, **49**, 3, DOI: 10.1007/s10511-006-0002-6
- Kawabata, K. S., Akitaya, H., Yamanaka, M., et al., Optical and Near-infrared Polarimetry of Highly Reddened Type Ia Supernova 2014J: Peculiar Properties of Dust in M82. 2014, *Astrophys. J., Lett.*, **795**, L4, DOI: 10.1088/2041-8205/795/1/L4
- Kessler, R., Becker, A. C., Cinabro, D., et al., First-Year Sloan Digital Sky Survey-II Supernova Results: Hubble Diagram and Cosmological Parameters. 2009, *Astrophys. J., Suppl.*, **185**, 32, DOI: 10.1088/0067-0049/185/1/32
- Marion, G. H., Sand, D. J., Hsiao, E. Y., et al., Early Observations and Analysis of the Type Ia SN 2014J in M82. 2015, *Astrophys. J.*, **798**, 39, DOI: 10.1088/0004-637X/798/1/39
- Phillips, M. M., The absolute magnitudes of Type IA supernovae. 1993, *Astrophys. J., Lett.*, **413**, L105, DOI: 10.1086/186970
- Phillips, M. M., Lira, P., Suntzeff, N. B., et al., The Reddening-Free Decline Rate Versus Luminosity Relationship for Type IA Supernovae. 1999, *Astron. J.*, **118**, 1766, DOI: 10.1086/301032
- Poznanski, D., Ganeshalingam, M., Silverman, J. M., & Filippenko, A. V., Low-resolution sodium D absorption is a bad proxy for extinction. 2011, *Mon. Not. R. Astron. Soc.*, **415**, L81, DOI: 10.1111/j.1745-3933.2011.01084.x
- Prieto, J. L., Rest, A., & Suntzeff, N. B., A New Method to Calibrate the Magnitudes of Type Ia Supernovae at Maximum Light. 2006, *Astrophys. J.*, **647**, 501, DOI: 10.1086/504307
- Pskovskii, I. P., Light curves, color curves, and expansion velocities of Type I supernovae as functions of the rate of brightness decline. 1977, *Astron. Zh.*, **54**, 1188

- Richmond, M. W., Treffers, R. R., Filippenko, A. V., & Paik, Y., UBVRI Photometry of SN 1993J in M81: Days 3 to 365. 1996, *Astron. J.*, **112**, 732, DOI: 10.1086/118048
- Riess, A. G., Filippenko, A. V., Challis, P., et al., Observational Evidence from Supernovae for an Accelerating Universe and a Cosmological Constant. 1998, *Astron. J.*, **116**, 1009, DOI: 10.1086/300499
- Schlafly, E. F. & Finkbeiner, D. P., Measuring Reddening with Sloan Digital Sky Survey Stellar Spectra and Recalibrating SFD. 2011, *Astrophys. J.*, **737**, 103, DOI: 10.1088/0004-637X/737/2/103
- Srivastav, S., Ninan, J. P., Kumar, B., et al., Optical and NIR observations of the nearby type Ia supernova SN 2014J. 2016, *Mon. Not. R. Astron. Soc.*, **457**, 1000, DOI: 10.1093/mnras/stw039
- Stanishev, V., Goobar, A., Benetti, S., et al., SN 2003du: 480 days in the life of a normal type Ia supernova. 2007, *Astron. Astrophys.*, **469**, 645, DOI: 10.1051/0004-6361:20066020
- Stritzinger, M., Hamuy, M., Suntzeff, N. B., et al., Optical Photometry of the Type Ia Supernova 1999ee and the Type Ib/c Supernova 1999ex in IC 5179. 2002, *Astron. J.*, **124**, 2100, DOI: 10.1086/342544
- Tsvetkov, D. Y., Metlov, V. G., Shugarov, S. Y., Tarasova, T. N., & Pavlyuk, N. N., Supernova 2014J at maximum light. 2014, *Contributions of the Astronomical Observatory Skalnate Pleso*, **44**, 67
- Tsvetkov, D. Y., Shugarov, S. Y., Volkov, I. M., et al., Optical observations of SN 2011fe. 2013, *Contributions of the Astronomical Observatory Skalnate Pleso*, **43**, 94
- Turatto, M., Benetti, S., & Cappellaro, E., Variety in Supernovae. 2003, in *From Twilight to Highlight: The Physics of Supernovae*, ed. W. Hillebrandt & B. Leibundgut, 200
- Wang, X., Filippenko, A. V., Ganeshalingam, M., et al., Improved Distances to Type Ia Supernovae with Two Spectroscopic Subclasses. 2009a, *Astrophys. J., Lett.*, **699**, L139, DOI: 10.1088/0004-637X/699/2/L139
- Wang, X., Li, W., Filippenko, A. V., et al., The Golden Standard Type Ia Supernova 2005cf: Observations from the Ultraviolet to the Near-Infrared Wavebands. 2009b, *Astrophys. J.*, **697**, 380, DOI: 10.1088/0004-637X/697/1/380
- Wang, X., Li, W., Filippenko, A. V., et al., Optical and Near-Infrared Observations of the Highly Reddened, Rapidly Expanding Type Ia Supernova SN 2006X in M100. 2008, *Astrophys. J.*, **675**, 626, DOI: 10.1086/526413
- Zheng, W., Shivvers, I., Filippenko, A. V., et al., Estimating the First-light Time of the Type Ia Supernova 2014J in M82. 2014, *Astrophys. J., Lett.*, **783**, L24, DOI: 10.1088/2041-8205/783/1/L24